



PII: S0017-9310(96)00390-0

# Simple models of spectral radiative properties of carbon dioxide

Y. U. KHAN,† D. A. LAWSON‡ and R. J. TUCKER§

† School of Mathematical and Information Sciences, Coventry University, Coventry CV1 5FB, U.K.

§ Gas Research Centre, British Gas plc, Loughborough, LE11 3QU, U.K.

(Received 22 November 1995 and in final form 5 December 1996)

**Abstract**—Spectral properties of pure carbon dioxide are thoroughly investigated in the gas temperature range 600–2400 K and  $P_aL$  range of 0.01–10 atm m. Regression modelling of spectral band properties (absorption coefficient ( $k_i$ ), lower ( $\lambda_{l,i}$ ) and upper ( $\lambda_{u,i}$ ) wavelength limits) derived from an Edwards wide band model is carried out. Comparisons of the regression models in a banded zone method and a weighted sum of grey gases model for carbon dioxide with Edwards wide band model are presented which show that good agreement has been achieved for the regression model. © 1997 Elsevier Science Ltd.

## INTRODUCTION

In many high temperature processes radiation is the dominant mode of heat transfer. In such situations an accurate representation of the radiative heat transfer phenomenon can be important in making accurate predictions of overall heat transfer.

Many applications of interest (for example, rocket and aircraft propulsion, boilers, furnaces) involve combustion products from hydrocarbon fuels at high temperatures. In these situations the gas to gas and gas to surface wall radiative heat transfer is of great importance. The main contributors of gas emission/absorption from these combustion products are carbon dioxide (CO<sub>2</sub>) and water vapour (H<sub>2</sub>O). The emission/absorption of these gases does not extend continuously over the whole wavelength spectrum as does that of a solid surface. Instead emission/absorption of radiation is restricted to specific regions of the wavelength spectrum.

Radiation in a spectral band depends on the spectral lines that lie within that band. The accuracy of the predicted heat fluxes increases as these bands become narrower. Exact results are only achieved from line by line calculations, but it is difficult to determine the spectral emissivity/absorptivity of the band this way because of the complexity of the calculations involved. The complexity arises because of the rapid variation (with respect to the wavelength) of the absorption coefficients of lines in the band. This complicated spectral behaviour of combustion products must be represented if accurate radiative heat transfer calculations are to be carried out. In this paper, the

spectral behaviour of pure carbon dioxide is studied.

The zone method [1] is a well-established method for determining radiative heat transfer calculations in enclosures where radiation is the dominant mode of heat transfer. This method has a long and well-established pedigree and has been used successfully in a range of applications, notably furnaces and other high temperature heating plants [2–4].

In the zone method the emitting/absorbing medium and the enclosure surfaces are assumed to be grey. Recent work [5] has shown how to extend Hottel's method to deal with spectrally dependent properties by dividing the wavelength domain into a finite number of bands and treating properties within each band as grey.

In this paper we present simple models for calculating spectral properties of carbon dioxide (a common constituent in combustion products). These properties can then be used in a banded zone method to determine overall radiative heat transfer.

In the next section the basic ideas of the zone method are described. Following this a brief survey of models of the non-grey behaviour of gases is given. The Edwards wide band model (EWBM) is probably the most widely used method of determining gas properties. The key elements of this model are presented. This model is too computationally complex for routine inclusion in the zone method calculations and so simple regression fits of carbon dioxide properties for the temperature range 600–2400 K and  $P_aL$  range 0.01–10 atm m have been generated. Some sample calculations using the regression models and a weighted sum of grey gases model (WSGGM) for carbon dioxide are compared with results obtained using the full EWBM. These are shown to be in good agreement.

† Author to whom correspondence should be addressed.

### NOMENCLATURE

$a$	weighting coefficient of WSGGM	$T$	temperature
$A$	area of surface	$V$	gas volume.
$b$	grey gases coefficients of WSGGM	Greek symbols	
$F$	fraction of total blackbody emissive power	$\varepsilon$	emissivity
$\overline{GG}$	gas-gas total exchange area	$\lambda$	wavelength
$\overline{GG}$	gas-gas direct flux area	$\sigma$	Stefan-Boltzmann constant
$\overline{GS}$	gas-surface total exchange area	$\tau$	gas transmissivity.
$\overline{GS}$	gas-surface direct flux area	Subscripts	
$k$	absorption coefficient	$a$	absorbing gas
$K$	attenuation coefficient	$g$	gas volume zone
$L$	mean beam length	$i$	spectral band number
$P$	total gas pressure	$j$	grey gas number in WSGGM
$Q$	heat flux	$l$	lower wavelength limit
$R^2$	variation percentage	$m$	volume zone number
$s$	standard deviation	$n$	surface zone number
$\overline{SG}$	surface-gas total exchange area	$s$	surface zone
$\overline{SG}$	surface-gas direct flux area	$t$	total
$\overline{SS}$	surface-surface total exchange area	$u$	upper wavelength limit.
$\overline{SS}$	surface-surface direct flux area		

### HOTTEL'S ZONE METHOD

In this method, the enclosure surfaces and gas volume are divided into a finite number of surface and volume zones. Each gas zone is assumed to be isothermal and have uniform radiative properties. The surfaces are considered to be diffuse grey emitters. An energy balance is written for each zone and the radiation exchange among all the surface and volume zones is then calculated.

Central to the zone method are exchange areas. Direct exchange areas (DEAs) give a measure of the amount of radiation emitted by one zone which is directly intercepted by another zone. Total exchange areas (TEAs) are a measure of the amount of the radiation emitted by one zone which is eventually absorbed by another zone.

DEAs and TEAs are calculated from the geometric orientation of the zones, the gas attenuation coefficient and surface emissivities. For a given attenuation coefficient the DEAs and TEAs are independent of the gas zone temperatures. Hence, they need only be calculated once before solving the zone energy balance equations for temperatures and heat fluxes. These equations are formulated for the radiation interchanges between all surface to surface, surface to volume, volume to surface and volume to volume zones. From these equations the heat fluxes are calculated.

The standard zone method [1] requires the gas to be grey. In other words there is a single gas attenuation coefficient across the entire spectrum. Recent work [5] has shown that spectral effects can be represented by dividing the spectrum into a number of bands each of

which is treated as grey. The zone method can then be applied to each band.

Suppose that in a furnace enclosure, we have  $N$  surface zones and  $M$  gas volume zones. Then energy balances for surface and volume zones in the  $i$ th spectral region are given by

$$Q_{si} = \varepsilon_s A_s F_{si} \sigma T_s^4 - \sum_{n=1}^N (\overline{S_n S_s})_i F_{ni} \sigma T_n^4 - \sum_{m=1}^M (\overline{G_m S_s})_i F_{mi} \sigma T_m^4$$

$$Q_{gi} = 4K_g V_g F_{gi} \sigma T_g^4 - \sum_{n=1}^N (\overline{S_n G_g})_i F_{ni} \sigma T_n^4 - \sum_{m=1}^M (\overline{G_m G_g})_i F_{mi} \sigma T_m^4$$

where  $Q_{si}$  is the  $i$ th spectral band heat flux for the  $s$ th surface zone and  $Q_{gi}$  is the  $i$ th spectral band heat flux for the  $g$ th volume zone. The  $(\overline{S_n S_s})_i$  is the TEA from surface zone  $S_n$  to  $S_s$ ,  $(\overline{S_n G_g})_i$  is the TEA from surface zone  $S_n$  to volume zone  $G_g$  and  $(\overline{G_m G_g})_i$  is the TEA from volume zone  $G_m$  to  $G_g$ . The subscript  $i$  refers to the  $i$ th spectral band calculation. The expression  $F_{si}$  is given by

$$F_{si} = F_{\lambda_i T_s - \lambda_u T_s} = F_{0 - \lambda_u T_s} - F_{0 - \lambda_i T_s}$$

$F_{0 - \lambda T}$  is the fraction of the blackbody spectrum between wavelength 0 and  $\lambda$ . Terms of the form  $F_{0 - \lambda T}$  can be computed from an approximation of an infinite series [6].

### MODELS OF NON-GREY BEHAVIOUR

To model the non-grey properties of spectral regions of carbon dioxide, some authors use the grey gas approximation [7–9], weighted sum of grey gases model [10–12] or more accurate approaches [13–15] which take into account the discrete emission/absorption bands of the exponential wide band model [16]. A description of this model is given in the next section.

The concept of the weighted sum of grey gases was first presented within the framework of the zone method [1]. This method can be applied to arbitrary geometries with varying absorption coefficients, but is limited to gases within a grey walled enclosure. In this model, the non-grey gas is replaced by a number of grey gases, for which the heat transfer rates are calculated independently. Total fluxes are found from a weighted sum of the fluxes for each of the grey gases. The temperature dependent weighting coefficients are calculated from formulae fitted to data from EWBM. The weighted sum of grey gases model essentially only allows for variation with temperature in total gas properties (that is, properties integrated over the whole wavelength spectrum).

Band models represent the mean spectral emissivities/absorptivities in a small wavelength band by theoretical profiles. These are divided into two groups, narrow band models and wide band models. Narrow band models use information of individual line shapes, widths and spacings to derive band characteristics within a defined wavenumber interval. There are two different line arrangements for narrow band models used extensively in the literature. The Elsasser or regular model [17] assumes that the lines are of uniform intensity and are equally spaced. The Goody or statistical model [18] assumes a random exponential line intensity distribution and a random line position selected from a uniform probability distribution. A detailed discussion of the narrow band models has been given in [16, 19, 20]. Accurate predictions require the narrow band to have a width in wavenumbers of about  $25 \text{ cm}^{-1}$ . Therefore, the total intensity calculation for carbon dioxide requires calculation of about 300 narrow band regions. The complexity of narrow band models and the large amount of computational time which they require, make them unsuitable for most engineering combustion calculations.

The radiation emission/absorption characteristics for each band of any gas can be obtained from experiments and then relations can be fitted to this data. The assumed profile of the band absorption may be box or triangular shaped or an exponential function. The appropriate parameters are then selected using curve fitting. These kind of models are known as wide band models, and among them the EWBM is the most commonly used.

#### EDWARDS WIDE BAND MODEL (EWBM)

EWBM takes into consideration the weakly emitting/absorbing lines in the wings of the spectral bands

as the radiation path length increases. This model consists of emission/absorption lines with wavenumbers that form an array with exponentially decreasing line intensities moving away from the band centre. Narrow band spectral models typically require calculations in 300 bands. The EWBM requires only six bands. However, the computation required for each band is still considerable.

EWBM gives a reasonably accurate model for representing measurements of gas properties. Three parameters are necessary for a complete description of band absorption. These are the band width, line width and the integrated band intensity. Once these parameters are calculated for each spectral region the required gas properties (transmissivity and hence absorption coefficients and band limits) can be found.

The transmissivity values and wavelength limits for the individual bands are calculated using the EWBM. In the wavelength regions where the bands overlap, the band transmissivity is taken to be the product of overlapping bands. In the wavelength regions where there is no emission/absorption by the gas the transmissivity value is taken to be 1. The band absorption coefficients ( $k_i$ ) can be found from the band transmissivity values. For the  $i$ th spectral band transmissivity

$$\tau_i = e^{-k_i P_a L},$$

therefore,

$$k_i = -\frac{\log_e(\tau_i)}{P_a L}.$$

#### REGRESSION MODELLING PROCEDURE

A set of data for absorption coefficients ( $k_i$ ), lower ( $\lambda_{l,i}$ ) and upper ( $\lambda_{u,i}$ ) wavelength limits of all the spectral bands has been obtained from the EWBM. The calculations are carried out for pure carbon dioxide at  $P_a L$  values of 0.01, 0.05, 0.1, 0.5, 1, 5 and 10 atm m, where  $P_a$  is the participating gas (in this case  $\text{CO}_2$ ) partial pressure and  $L$  is an average of the path length travelled by radiation within the absorbing gas volume. The gas temperatures ( $T_g$ ) are taken at intervals of 100 K in the range 600–2400 K.

Data obtained from EWBM shows that the band absorption coefficients, the lower and upper limits are dependent on  $T_g$  and the product of participating gas partial pressures and mean beam length ( $P_a L$ ). The source temperatures have no effect on spectral band absorption coefficients, lower and upper wavelength limits. The data values for band absorption coefficient, lower and upper limits of these bands are regressionally modelled individually for each band against the  $T_g$  and  $P_a L$ . The comparison graphs of EWBM data against the values generated from the regression models are shown in Appendix A.

In the regression models the measure  $R^2\%$  gives the percentage of the variation in the data values that is accounted for by the fitted equation and  $s$  is the stan-

Table 1. Spectral band data at  $P_aL = 0.133$  atm m and  $T_g = 1000$  K

Lower limit $\lambda_l$ $\mu\text{m}$	Upper limit $\lambda_u$ $\mu\text{m}$	Band absorptivity $\alpha_i$	Block fraction $\alpha_{g,i}$	Block fraction % $\alpha_{g,i}$
1.91	1.94	0.1	0.00083	0.92
2.62	2.85	0.60474	0.037	40.86
4.15	4.67	0.84382	0.04425	48.90
9.17	9.72	0.1	0.00054	0.59
10.10	10.76	0.1	0.00047	0.51
12.84	18.05	0.76707	0.00746	8.24
			$\alpha_g = 0.09054$	

standard deviation of the data values about the regression line (the standard error estimate). This value can also be thought of as a measure of how much the observed values differ from the fitted values.

#### Regression modelling of carbon dioxide

For  $\text{CO}_2$  there are six spectral bands that emit/absorb most of the radiation in the entire wavelength range. The data obtained from Ref. [16] shows that more than 95% of radiative heat exchange occurs in 2.7, 4.3 and 15  $\mu\text{m}$  bands for the  $P_aL < 0.25$  atm m and 2, 2.7, 4.3 and 15  $\mu\text{m}$  bands for the  $P_aL \geq 0.25$  atm m.

For the gas temperature of 1000 K and source temperature of 1500 K, the block fraction % $\alpha_{g,i}$  in comparison to total absorption  $\alpha_j$  at  $P_aL = 0.133$  atm m is given in Table 1 and spectral band absorptivity  $\alpha_i$  graphically represented in Fig. 1. For the same gas and source temperature values the block fraction % $\alpha_{g,i}$  in comparison to total absorption  $\alpha_g$  at  $P_aL = 1.33$  atm m is given in Table 2 and spectral band absorptivity  $\alpha_i$  graphically represented in Fig. 2.

Figure 1 shows that at  $P_aL = 0.133$  atm m 98% of the radiation is passing through 2.7, 4.3 and 15  $\mu\text{m}$  bands whereas Fig. 2 shows that at  $P_aL = 1.33$  atm m 95% of the radiation is passing through 2, 2.7, 4.3 and

15  $\mu\text{m}$ . Therefore, these are the only spectral regions regressionally modelled and any other spectral bands are ignored because of their negligible effect. All four bands are modelled in the  $P_aL$  range (0.01–10) atm m except the 2  $\mu\text{m}$  band which is only significant for  $P_aL \geq 0.25$  atm m.

2  $\mu\text{m}$  band (from 0.25 atm m to 10 atm m).

$$e^{k_2} = 1.01 - 0.000015T_g + \frac{0.133}{P_aL}$$

$$+ 0.0443 \log_e(P_aL)$$

$$\lambda_{l,2} = 1.86 - 0.000017T_g - 0.0359 \log_e(P_aL)$$

$$+ 0.0144(\log_e(P_aL))^2$$

$$\lambda_{u,2} = 1.99 + 0.00002T_g + 0.0449 \log_e(P_aL)$$

$$- 0.0185(\log_e(P_aL))^2$$

	$e^{k_2}$	$\lambda_{l,2}$	$\lambda_{u,2}$
$R^2\%$	86.9	73.5	75.1
$s$	0.0222	0.01363	0.01591

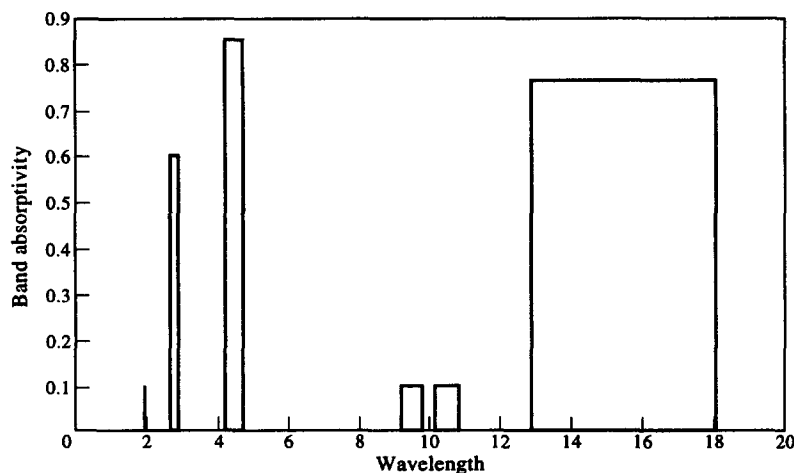
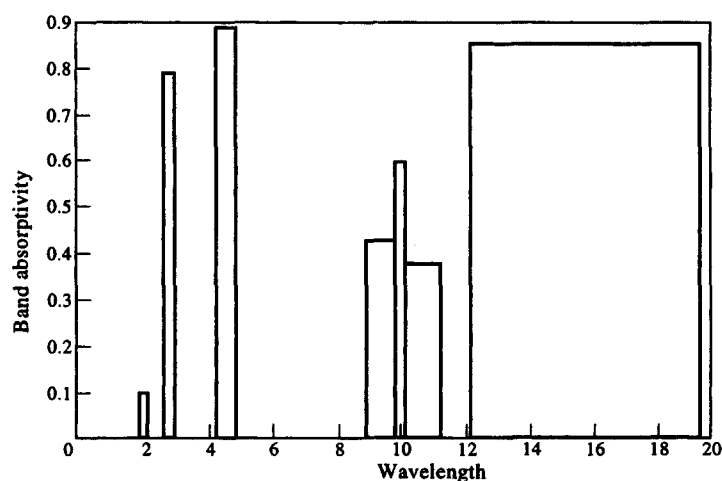


Fig. 1. Spectral band data at  $P_aL = 0.133$  atm m and  $T_g = 1000$  K.

Table 2. Spectral band data at  $P_a L = 1.33$  atm m and  $T_g = 1000$  K

Lower limit $\lambda_l \mu\text{m}$	Upper limit $\lambda_u \mu\text{m}$	Band absorptivity $\alpha_i$	Block fraction $\alpha_{g,i}$	Block fraction % $\alpha_{g,i}$
1.81	2.05	0.1	0.00834	5.29
2.57	2.91	0.793	0.07061	44.83
4.15	4.85	0.885	0.05941	37.72
8.87	9.77	0.393	0.00363	2.31
9.77	10.07	0.601	0.00153	0.97
10.07	11.17	0.343	0.0025	1.59
12.15	19.57	0.848	0.0115	7.30
			$\alpha_g = 0.15751$	

Fig. 2. Spectral band data at  $P_a L = 1.33$  atm m and  $T_g = 1000$  K.*2.7  $\mu\text{m}$  band.*

$$\log_e(k_{2.7}) = 0.657 - 0.000168T_g - 0.761 \log_e(P_a L) - 0.0695(\log_e(P_a L))^2$$

$$\lambda_{l,2.7} = 2.67 - 0.00294\sqrt{T_g} - 0.0219 \log_e(P_a L)$$

$$\lambda_{u,2.7} = 2.86 + 0.000053T_g + 0.0276 \log_e(P_a L)$$

	$\log_e(k_{2.7})$	$\lambda_{l,2.7}$	$\lambda_{u,2.7}$
$R^2\%$	99.4	93	91.4
$s$	0.121	0.01578	0.02249

*4.3  $\mu\text{m}$  band.*

$$\log_e(k_{4.3}) = 0.839 - 0.000103T_g - 0.904 \log_e(P_a L)$$

$$\lambda_{l,4.3} = 4.15$$

$$\lambda_{u,4.3} = 4.62 + 0.000212T_g + 0.0954 \log_e(P_a L)$$

	$\log_e(k_{4.3})$	$\lambda_{l,4.3}$	$\lambda_{u,4.3}$
$R^2\%$	99.9	100	95.4
$s$	0.07972	0	0.05736

*15  $\mu\text{m}$  band.*

$$\log_e(k_{15}) = 1.1 - 0.000272T_g - 0.862 \log_e(P_a L) - 0.066(\log_e(P_a L))^2$$

$$\lambda_{l,15} = 13 - 0.000672T_g - 0.221 \log_e(P_a L)$$

$$\lambda_{l,15}^+ = 13.7 + 0.000046T_g + 2.62(P_a L)$$

$$- 0.114\sqrt{(T_g \times P_a L)}$$

$$\lambda_{l,15}^* = 40.6 + 0.00277T_g + 0.58(P_a L)$$

$$- 4.01 \log_e(T_g \times P_a L) - \frac{1.6}{(P_a L)^2}$$

$$\lambda_{u,15} = 16.2 + 0.00243(T_g) + 0.88 \log_e(P_a L)$$

$$+ 0.198(\log_e(P_a L))^2$$

	$\log_e(k_{15})$	$\lambda_{l,15}$	$\lambda_{l,15}^+$	$\lambda_{l,15}^*$	$\lambda_{u,15}$
$R^2\%$	97.2	86.4	77.9	91.3	76.4
$s$	0.2981	0.2293	0.3876	0.3764	1.145

$\lambda_{l,15}$  is fitted for the gas temperature of 600–1400 K over the entire  $P_a L$  range.

$\lambda_{i,15}^+$  is fitted for the gas temperature of 1400–2400 K over the  $P_a L < 0.25$  atm m.

$\lambda_{i,15}^*$  is fitted for the gas temperature of 1400–2400 K over the  $P_a L \geq 0.25$  atm m.

**WEIGHTED SUM OF GREY GASES MODEL (WSGGM)**

This model is usually used to calculate carbon dioxide total emissivity ( $\epsilon_g$ ). The carbon dioxide gas is replaced by a number (=7 in this case) of grey gases each of which have a constant absorption coefficient ( $k_j$ ) which is independent of wavelength and temperature [21]. The temperature dependence is carried out by the weighting coefficients  $a_j(T_g)$  generally expressed as a low-order polynomial in  $T_g$ . The total emissivity of carbon dioxide is calculated as

$$\epsilon_g = \sum_{j=1}^7 a_j(T_g)[1 - e^{-k_j P_a L}].$$

The value of  $a_j(T_g)$  is always positive for all the grey gases involved and the following condition must also be obeyed

$$\sum_{j=1}^7 a_j(T_g) = 1$$

The absorption coefficient for  $k_1 = 0$  in Table 3 because this clear gas (gas that does not emit/absorb any radiation) accounts for the windows in the carbon dioxide emitting/absorbing spectral bands. Using the coefficients in Table 3 it is possible to calculate the total carbon dioxide emissivity at any  $T_g$  and  $P_a L$ , but for our purpose the individual grey gas attenuation coefficients ( $K_j = k_j \times P_a$ ) are found from the absorption coefficients ( $k_j$ ). Therefore, the DEAs and TEAs are calculated for all the zones using all the grey gas attenuation coefficients. Suppose that the TEAs for the  $j$ th absorption coefficient are  $(\overline{S_n S_s})_{K_j}$ ,  $(\overline{S_n G_g})_{K_j}$ ,  $(\overline{G_g S_n})_{K_j}$  and  $(\overline{G_m G_g})_{K_j}$ , respectively. Then the direct flux-areas (DFAs) are defined as

$$\overline{S_n S_s} = \sum_{j=1}^7 a_j(T_n)(\overline{S_n S_s})_{K_j}$$

Table 3. Grey gases coefficients for carbon dioxide WSGGM [21]

$j$	$b_{1,j}$	$b_{2,j}$	$b_{3,j}$	$k_j$ m <sup>-1</sup> atm <sup>-1</sup>
1	0.7280526	-0.044035	0.0033955	0.0
2	0.1074	-0.10705	0.072727	0.03647
3	0.027237	0.10127	-0.043773	0.3633
4	0.058438	-0.001208	0.0006558	3.10
5	0.019078	0.037609	-0.015424	14.96
6	0.056993	-0.025412	0.0026167	103.61
7	0.0028014	0.038826	-0.020198	780.7

$$\overline{S_n G_g} = \sum_{j=1}^7 a_j(T_n)(\overline{S_n G_g})_{K_j}$$

$$\overline{G_g S_n} = \sum_{j=1}^7 a_j(T_g)(\overline{G_g S_n})_{K_j}$$

$$\overline{G_m G_g} = \sum_{j=1}^7 a_j(T_m)(\overline{G_m G_g})_{K_j}$$

The weighting coefficients in each case are given as follows

$$a_j(T) = b_{1,j} + b_{2,j} \frac{T}{1000} + b_{3,j} \left( \frac{T}{1000} \right)^2$$

where  $b_{1,j}$ ,  $b_{2,j}$  and  $b_{3,j}$  are the coefficients from the WSGGM in Table 3.

The overall heat flux for any surface zone  $s$  and volume zone  $g$  are given as

$$Q_s = \epsilon_s A_s \sigma T_s^4 - \sum_{n=1}^N (\overline{S_n S_s}) \sigma T_n^4$$

$$- \sum_{m=1}^M (\overline{G_m S_s}) \sigma T_m^4$$

$$Q_g = 4 \left( \sum_{j=1}^7 a_j(T_g) K_j \right) V_g \sigma T_g^4$$

$$- \sum_{n=1}^N (\overline{S_n G_g}) \sigma T_n^4 - \sum_{m=1}^M (\overline{G_m G_g}) \sigma T_m^4.$$

**SAMPLE CALCULATIONS**

Four sets of calculations at gas temperatures of 600, 1000, 1600 and 2000 K are carried out to test the regression modelling. In these sets of calculations, a cube enclosure of dimension  $2 \times 2 \times 2$  m is used which contains pure carbon dioxide at  $P_a L$  values of 0.01, 0.05, 0.1, 0.5, 1, 5 and 10 atm m, respectively. Each surface of the enclosure is considered as an individual surface zone and their emissivities and temperatures are taken to be 0.5 and 1400 K, respectively. The entire enclosure volume is considered to be a single volume zone. The direct exchange areas (DEAs) and total exchange areas (TEAs) are calculated using the RADEX [22] program. In these sets of calculations, the mean beam length  $L = 1.166667$  m is kept constant, but the gas partial pressure  $P_a$  is adjusted according to the desired  $P_a L$  values. The value of  $L$  is found by using the formula  $L = 3.5 V/A_t$ , where  $V$  is the volume of the gas enclosure and  $A_t$  is its total boundary surface area [6].

The regression models can be used for any gas temperatures ( $T_g$ ) and  $P_a L$  values in the range described above to obtain the relevant band absorption coefficients, lower and upper limits for individual spectral band calculations. The spectral absorption coefficients ( $k_i$ ) can be multiplied by the gas partial pressure to obtain a value for the spectral attenuation

coefficient ( $K_i$ ) that can be used in the zone method to calculate spectral radiative heat fluxes. These spectral radiative heat fluxes are summed over the entire wavelength range to obtain the total radiative heat flux values.

The results of the calculations are given in Tables 4–7. These show the calculated total heat flux out of the gas. In each table the EWBM column gives the results from calculations carried out using the Edwards wide band model properties (including all

bands, not just the four most important ones) that emit/absorb radiation at the given  $P_a L$  and gas temperature. The REGR column gives results from the calculations carried out using the fitted regression equations above to determine the absorption coefficients and wavelength limits of the spectral bands. The WSGGM column gives results from the calculations carried out using a weighted sum of grey gases model for carbon dioxide.

The percentage errors are calculated as

Table 4. Comparison of models at  $T_g = 600$  K

$P_a L$ atm m	$P_a$ atm	EWBM kW	REGR kW	WSGGM kW	Error 1 %	Error 2 %
0.01	0.00857	-115.0	-58.8	-132.3	-48.9	15.0
0.05	0.04286	-181.6	-145.6	-227.6	-19.8	25.3
0.1	0.08571	-213.6	-190.8	-278.6	-10.7	30.4
0.5	0.42857	-299.7	-310.2	-409.2	3.5	36.5
1	0.85714	-355.6	-369.2	-470.3	3.8	32.3
5	4.28571	-478.7	-523.8	-619.6	-9.4	29.4
10	8.57143	-536.8	-573.7	-681.2	6.9	26.9

Table 5. Comparison of models at  $T_g = 1000$  K

$P_a L$ atm m	$P_a$ atm	EWBM kW	REGR kW	WSGGM kW	Error 1 %	Error 2 %
0.01	0.00857	-79.8	-57.7	-95.6	-27.8	19.8
0.05	0.04286	-152.7	-125.7	-167.7	-17.7	9.8
0.1	0.08571	-182.3	-160.9	-206.6	-11.7	13.3
0.5	0.42857	-260.0	-254.7	-306.6	-2.0	17.9
1	0.85714	-304.5	-299.8	-353.7	-1.5	16.2
5	4.28571	-426.5	-421.9	-471.0	-1.1	10.4
10	8.57143	-471.1	-462.5	-521.0	-1.8	10.6

Table 6. Comparison of models at  $T_g = 1600$  K

$P_a L$ atm m	$P_a$ atm	EWBM kW	REGR kW	WSGGM kW	Error 1 %	Error 2 %
0.1	0.00857	52.4	52.9	64.6	0.8	23.3
0.05	0.04286	123.5	106.9	127.2	-13.4	3.0
0.1	0.08571	140.1	135.3	162.3	-3.4	15.8
0.5	0.42857	213.4	215.6	253.3	1.0	18.7
1	0.85714	260.6	248.7	296.6	-4.6	13.8
5	4.28571	386.1	362.7	417.6	-6.1	8.2
10	8.57143	434.0	402.3	478.0	-7.3	10.1

Table 7. Comparison of models at  $T_g = 2000$  K

$P_a L$ atm m	$P_a$ atm	EWBM kW	REGR kW	WSGGM kW	Error 1 %	Error 2 %
0.01	0.00857	175.1	205.3	139.2	17.3	-20.5
0.05	0.04286	417.5	403.5	380.0	-3.4	-9.0
0.1	0.08571	514.9	508.2	522.4	-1.3	1.5
0.5	0.42857	799.7	816.8	893.6	2.1	11.7
1	0.85714	977.6	944.5	1070.9	-3.4	9.5
5	4.28571	1534.0	1391.0	1649.3	-9.3	7.5
10	8.57143	1743.0	1563.0	1990.4	-10.3	14.2

$$\text{Error 1\%} = \left( \frac{\text{REGR}}{\text{EWBM}} - 1 \right) \times 100$$

$$\text{Error 2\%} = \left( \frac{\text{WSGGM}}{\text{EWBM}} - 1 \right) \times 100.$$

### CONCLUSION

Simple regression model for one of the main contributing gases to the thermal radiation in furnace enclosures has been developed. This model covers the gas temperature ( $T_g$ ) range 600–2400 K and path length partial pressure product ( $P_a L$ ) range 0.01–10 atm m. The result comparisons of REGR and WSGGM with EWBM have been carried out in Tables 4–7.

The heat flux results of REGR in comparison to EWBM are in good agreement for all the  $P_a L$  and  $T_g$  combinations (heat flux error less than 10%) except the large errors at low  $P_a L$  values (0.01–0.05 atm m) and low gas temperatures (600–1000 K). This occurs because the regression absorption coefficients at low  $P_a L$  values are undercalculated and, therefore, less heat radiation is absorbed (see graphs in Appendix A).

The heat flux results of WSGGM in comparison to EWBM are extremely over predicted at all  $P_a L$  values and low gas temperatures (heat flux error of almost 30% at  $T_g = 600$  K). Although the heat flux results obtained using WSGGM improve as  $T_g$  increases (heat flux error of approximately 10% at  $T_g = 2000$  K) the results of REGR are in much better agreement to EWBM than the WSGGM results at all gas temperatures and partial pressure path length products greater than 0.05 atm m.

Furthermore the regression model is also a computationally more efficient method of radiation analysis than the WSGGM since it uses fewer sets of exchange areas. The regression model calculations need at most five sets of exchange areas (one per gas spectral band) whilst the WSGGM requires seven sets of exchange areas (one per gas attenuation coefficient).

### REFERENCES

- Hottel, H. C. and Sarofim, A. F., *Radiative Transfer*. McGraw-Hill, New York, 1967.
- Steward, F. R. and Guruz, H. R., Mathematical simulation of an industrial boiler by the zone method analysis. *Heat Transfer in Flames*, eds. N. H. Afgan and J. M. Beer, Scripta, Washington, 1974, pp. 47–71.
- Vercammen, A. J. and Froment, G. F., An improved zone method using Monte Carlo techniques for simulation of radiation in industrial furnaces. *International Journal of Heat and Mass Transfer*, 1980, **23**, 329–336.
- Elliston, D. G., Gray, W. A., Hibberd, D. F., Ho, T.-Y. and Williams, A., The effect of surface emissivity on furnace performance. *Journal of Institute of Energy*, 1987, **60**, 155–167.
- Khan, Y. U., Lawson, D. A. and Tucker, R. J., Radiative heat transfer calculations for non-grey surfaces. *Con-*

*ference—Numerical methods in Thermal Problems*, 1995, **IX**, 351–361.

- Siegel, R. and Howell, J. R., *Thermal Radiation Heat Transfer*. Hemisphere Publishing Corporation, Washington, 1992.
- Viskanta, R., Interaction of heat transfer by conduction, convection and radiation in radiating fluid. *Journal of Heat Transfer*, 1963, **85**(2), 318–328.
- Kurosaki, Y., Heat transfer by simultaneous radiation and convection in an absorbing and emitting medium in a flow between parallel plates. *Fourth International Heat Transfer Conference*, 1984, **III**, paper R2.5.
- Chung, T. J. and Kim, J. Y., Two-dimensional, combined-mode heat transfer by conduction, convection and radiation in emitting, absorbing and scattering media—solution by finite elements. *Journal of Heat Transfer*, 1984, **106**, 448–452.
- Modest, M. F., The weighted sum of grey gases model for arbitrary solution methods in radiative transfer. *ASME Journal of Heat Transfer*, 1991, **113**, 650–656.
- Denison, M. K. and Webb, B. W.,  $k$ -distribution and weighted sum of grey gases. A hybrid model. *10th International Heat Transfer Conference*, Brighton, 19–24, 1994.
- Taylor, P. B. and Foster, P. J., The total emissivities of luminous and non-luminous flames. *ASME Journal of Heat Transfer*, 1974, **17**, 1591–1605.
- Soto, S. D., Coupled radiation, conduction and convection in entrance region flows. *International Journal of Heat and Mass Transfer*, 1968, **11**, 39–54.
- Kim, D. M. and Viskanta, R., Interaction of convection and radiation heat transfer in high pressure and temperature steam. *International Journal of Heat and Mass Transfer*, 1984, **27**, 939–941.
- Habib, I. S. and Greif, R., Heat transfer to a flowing non-gray radiating gas: an experimental and theoretical study. *International Journal of Heat and Mass Transfer*, 1970, **13**, 1571–1582.
- Edwards, D. K., Molecular gas band radiation. *Advances in Heat Transfer* (eds T. F. Irvine and J. P. Hartnett), Vol. 12. Academic Press, New York, 1976, pp. 115–193.
- Elsasser, W. M., *Heat Transfer by Infrared Radiation in the Atmosphere*. Harvard Meteorological Studies no. 6. Harvard University Press, Cambridge, 1942.
- Goody, R. M., *Atmospheric Radiation, Theoretical Basis*, Vol. 1. Clarendon Press, Oxford 1964.
- Ludwig, C. B., Malkmus, W., Reardon, J. G. and Thomson, J. A. L., *A Handbook of Infrared Radiation from Combustion Gases*. NASA SP-3080, Washington D.C., 1973.
- Tien, C. L., *Advances in Heat Transfer* (eds T. F. Irvine and J. P. Hartnett), Vol. 5. Academic Press, New York, 1970, pp. 254–324.
- Farag, I. H., Non luminous gas radiation: approximate emissivity models. In *Proceedings of 7th Heat Transfer Conference*, 1982, **2**.
- Lawson, D. A., *RADEX: A User Guide*. Coventry University Research Report, 1993.

### APPENDIX A

#### Comparison graphs

The graph lines are of the following nature:

Original absorption coefficient = solid line  
 Regressional absorption coefficient = dotted line

Original lower wavelength limit = solid line  
 Regressional lower wavelength limit = dotted line  
 Original upper wavelength limit = dashed line  
 Regressional upper wavelength limit = dash-dotted line.



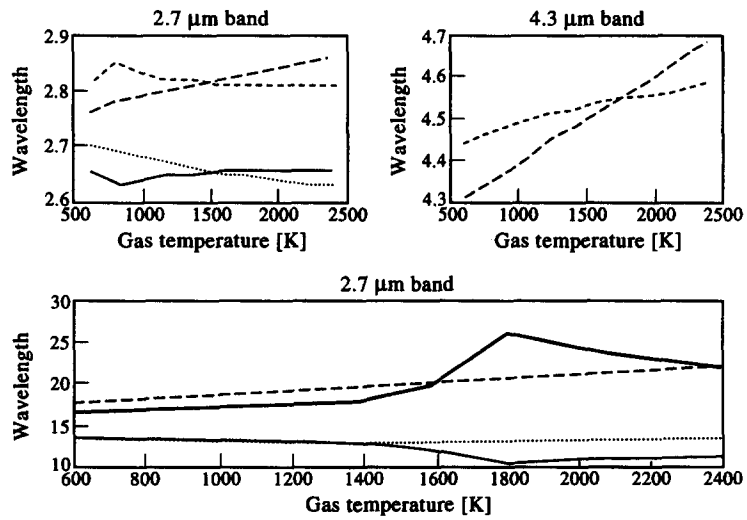


Fig. A1.  $PL = 0.01$  atm m : upper and lower limits in spectral bands.

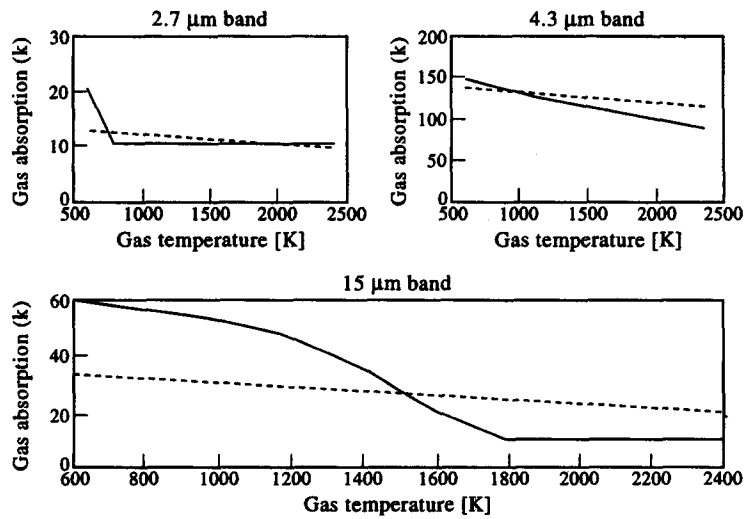


Fig. A2.  $PL = 0.01$  atm m : absorption coefficient in spectral bands.

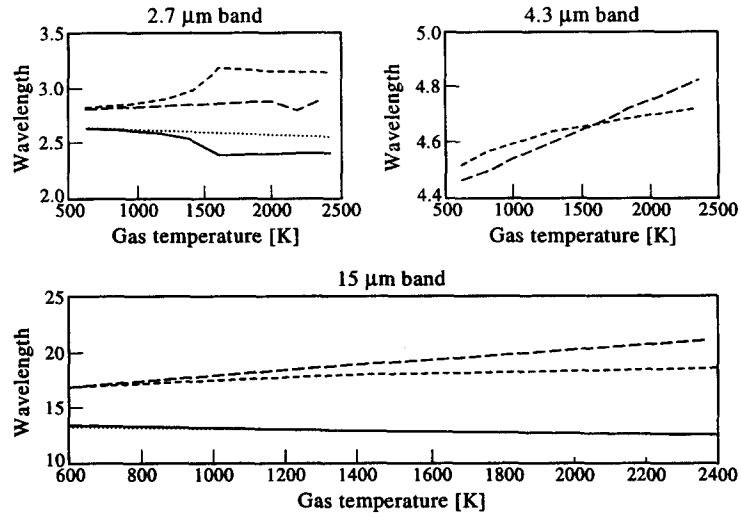


Fig. A3.  $PL = 0.05 \text{ atm m}$ : upper and lower limits in spectral bands.

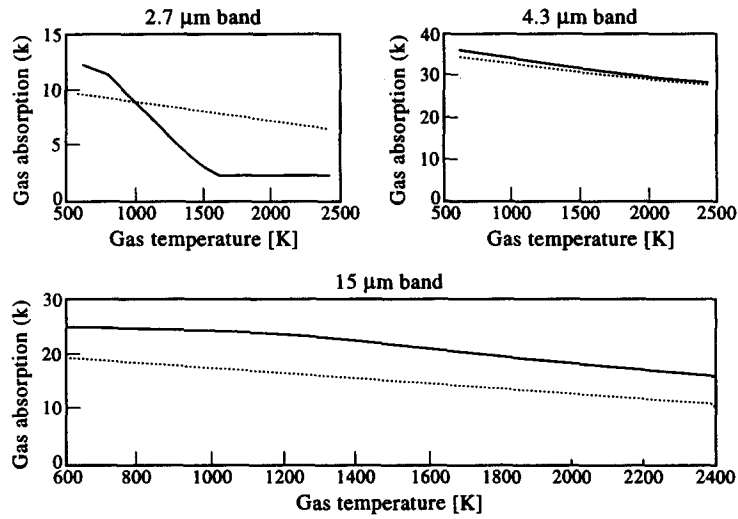


Fig. A4.  $PL = 0.05 \text{ atm m}$ : absorption coefficient in spectral bands.

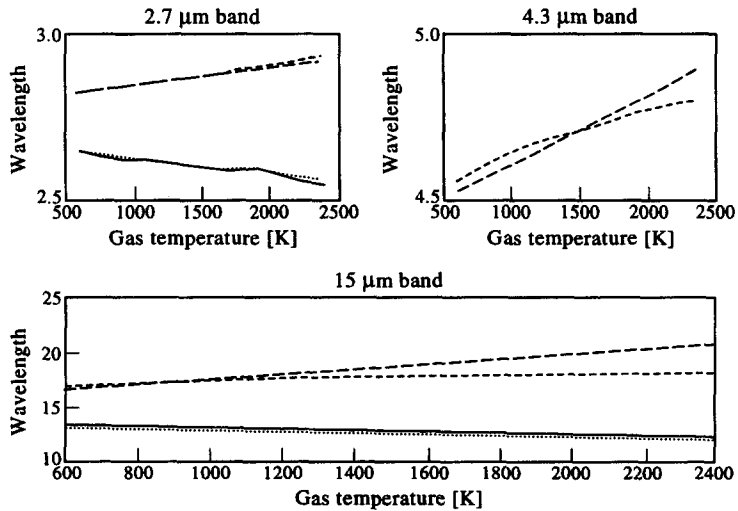
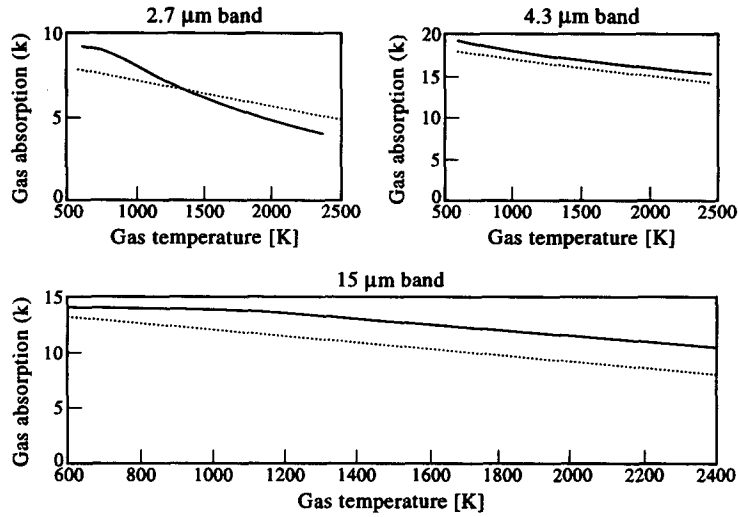
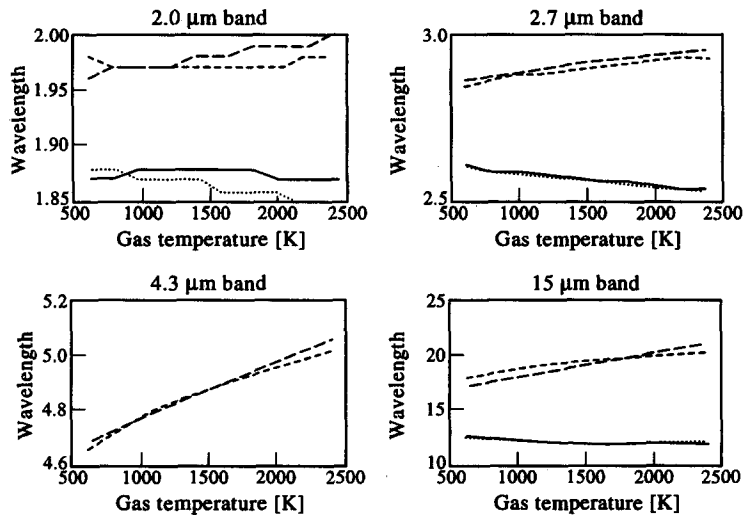
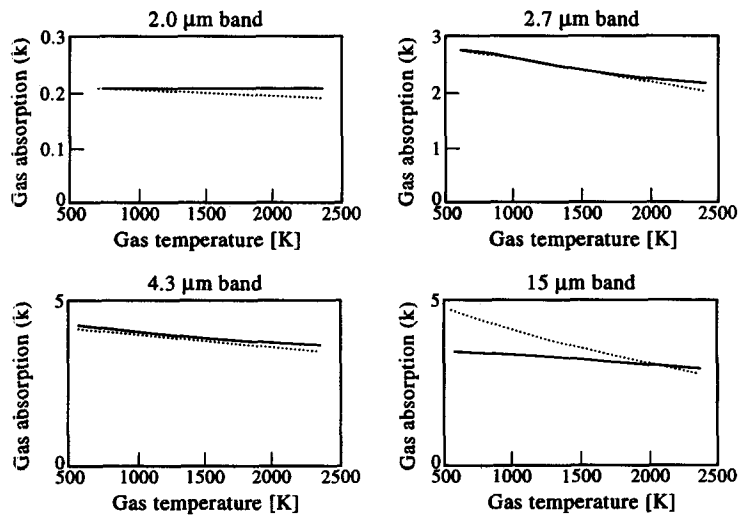


Fig. A5.  $PL = 0.1 \text{ atm m}$ : upper and lower limits in spectral bands.

Fig. A6.  $PL = 0.1$  atm m : absorption coefficient in spectral bands.Fig. A7.  $PL = 0.5$  atm m : upper and lower limits in spectral bands.Fig. A8.  $PL = 0.5$  atm m : absorption coefficient in spectral bands.

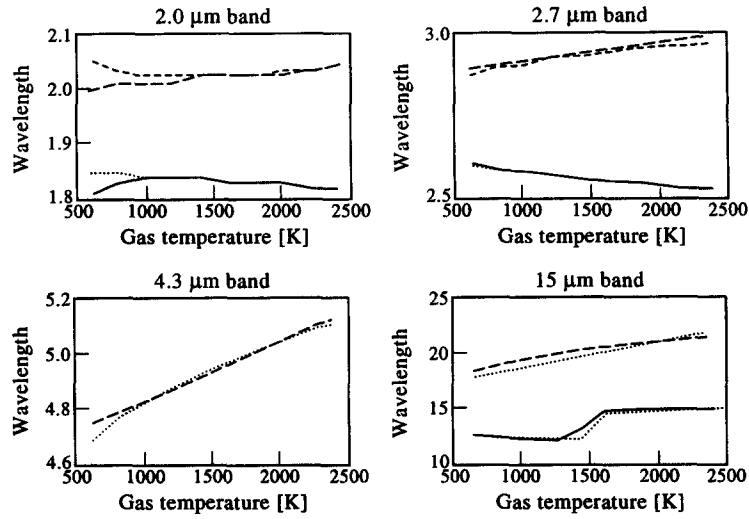


Fig. A9.  $PL = 1$  atm m: upper and lower limits in spectral bands.

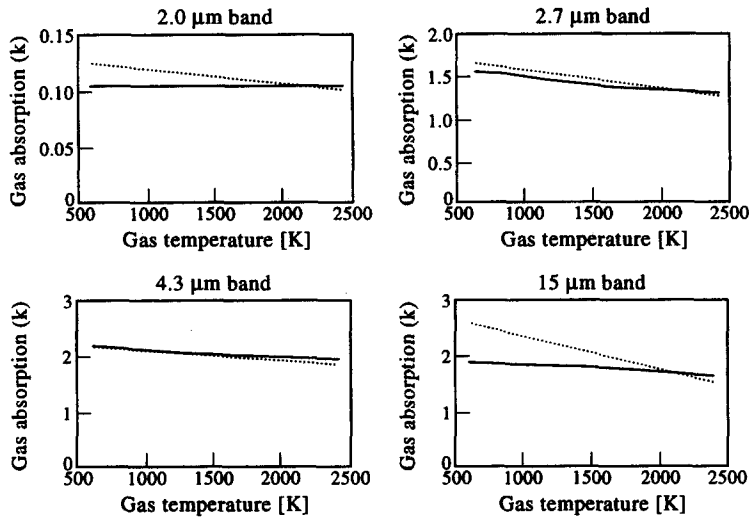


Fig. A10.  $PL = 1$  atm m: absorption coefficient in spectral bands.

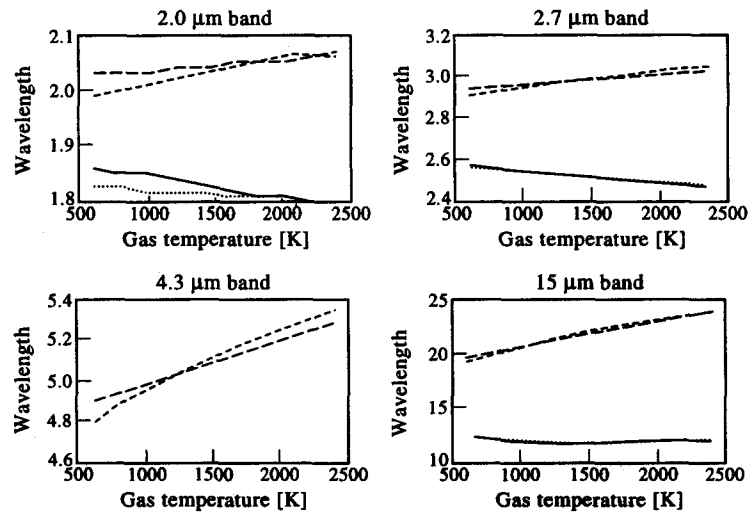
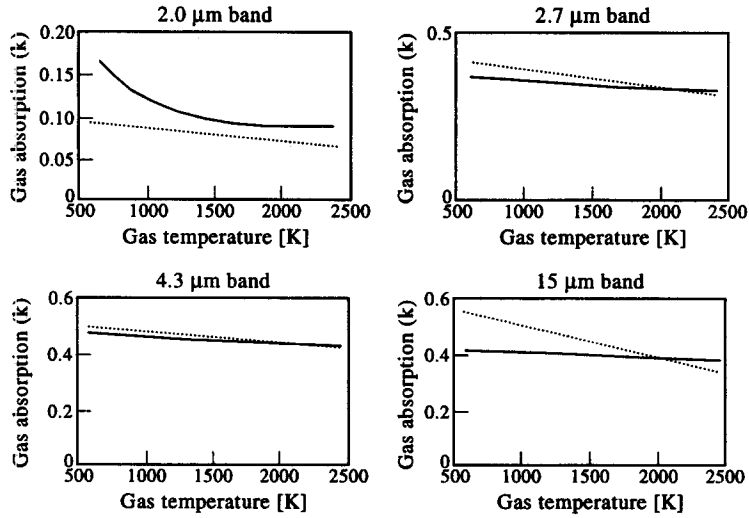
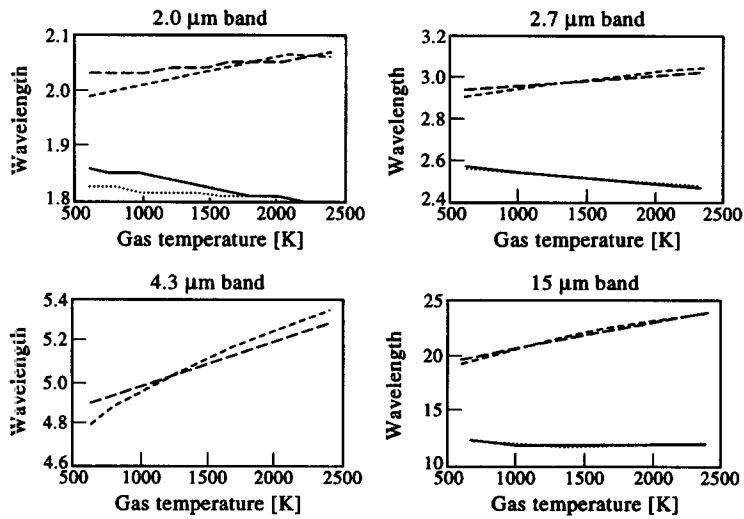
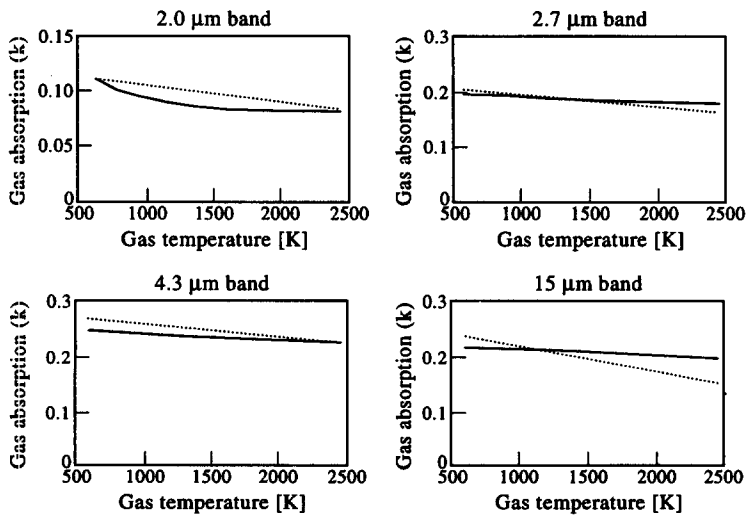


Fig. A11.  $PL = 5$  atm m: upper and lower limits in spectral bands.

Fig. A12.  $PL = 5$  atm m: absorption coefficients in spectral bands.Fig. A13.  $PL = 10$  atm m: upper and lower limits in spectral bands.Fig. A14.  $PL = 10$  atm m: absorption coefficient in spectral bands.